X-RAY AND NEAR-INFRARED OBSERVATIONS OF THE OBSCURED ACCRETING PULSAR IGR J18179–1621

Citation: Nowak, M. A., A. Paizis, J. Rodriguez, S. Chaty, M. Del Santo, V. Grinberg, J. Wilms, P. Ubertini, and R. Chini. "X-RAY AND NEAR-INFRARED OBSERVATIONS OF THE OBSCURED ACCRETING PULSAR IGR J18179–1621." The Astrophysical Journal 757, no. 2 (September 12, 2012): 143. © 2012 The American Astronomical Society

As Published: http://dx.doi.org/10.1088/0004-637x/757/2/143

Publisher: IOP Publishing

Persistent URL: http://hdl.handle.net/1721.1/95463

Version: Final published version: final published article, as it appeared in a journal, conference proceedings, or other formally published context

The Astrophysical Journal, 757:143 (8pp), 2012 October 1 doi:10.1088/0004-637X/757/2/143

X-RAY AND NEAR-INFRARED OBSERVATIONS OF THE OBSCURED ACCRETING PULSAR IGR J18179−1621

M. A. Nowak[1], A. Paizis[2], J. Rodriguez[3], S. Chaty[3,4], M. Del Santo[5], V. Grinberg[6], J. Wilms[6], P. Ubertini[5], and R. Chini[7,8]
[1] Massachusetts Institute of Technology, Kavli Institute for Astrophysics, Cambridge, MA 02139, USA; mnowak@space.mit.edu
[2] Istituto Nazionale di Astrofisica, INAF-IASF, Via Bassini 15, I-20133 Milano, Italy; ada@iasf-milano.inaf.it
[3] AIM-Astrophysique, Instrumentation et Modélisation (UMR-E 9005 CEA/DSM-CNRS-Université Paris Diderot)
Irfu/Service d'Astrophysique, Centre de Saclay FR-91191 Gif-sur-Yvette Cedex, France
[4] Institut Universitaire de France, 103, bd Saint-Michel, F-75005, Paris, France
[5] Istituto Nazionale di Astrofisica, INAF-IAPS, Via Fosso del Cavaliere 100, I-00133 Rome, Italy
[6] Dr. Karl Remeis-Sternwarte and Erlangen Centre for Astroparticle Physics, Universität Erlangen-Nürnberg, Sternwartstr. 7, D-96049 Bamberg, Germany
[7] Astronomisches Institut, Ruhr-Universität Bochum, Universitätsstraße 150, D-44780 Bochum, Germany
[8] Instituto de Astronomía, Universidad Católica del Norte, Avenida Angamos 0610, Casilla 1280, Antofagasta, Chile
Received 2012 June 3; accepted 2012 July 27; published 2012 September 12

ABSTRACT

IGR J18179−1621 is an obscured accreting X-ray pulsar discovered by *INTEGRAL* on 2012 February 29. We report on our 20 ks *Chandra*-High Energy Transmission Gratings Spectrometer observation of the source performed on 2012 March 17, on two short contemporaneous *Swift* observations, and on our two near-infrared (K_s, H_n, and J_n) observations performed on 2012 March 13 and 26. We determine the most accurate X-ray position of IGR J18179−1621, $\alpha_{\rm J2000} = 18^{\rm h}17^{\rm m}52\overset{\rm s}{.}18$, $\delta_{\rm J2000} = -16^\circ21'31\overset{''}{.}68$ (90% uncertainty of $0\overset{''}{.}6$). A strong periodic variability at 11.82 s is clearly detected in the *Chandra* data, confirming the pulsating nature of the source, with the light-curve softening at the pulse peak. The quasi-simultaneous *Chandra–Swift* spectra of IGR J18179−1621 can be well fit by a heavily absorbed hard power law ($N_{\rm H} = 2.2 \pm 0.3 \times 10^{23}$ cm^{-2} and photon index $\Gamma = 0.4 \pm 0.1$) with an average absorbed 2–8 keV flux of 1.4×10^{-11} erg cm^{-2} s^{-1}. At the *Chandra*-based position, a source is detected in our near-infrared (NIR) maps with $K_s = 13.14 \pm 0.04$ mag, $H_n = 16 \pm 0.1$ mag, and no J_n-band counterpart down to ∼18 mag. The NIR source, compatible with 2MASS J18175218−1621316, shows no variability between 2012 March 13 and 26. Searches of the UKIDSS database show similar NIR flux levels at epochs six months prior to and after a 2007 February 11 archival *Chandra* observation where the source's X-ray flux was at least 87 times fainter. In many ways IGR J18179−1621 is unusual: its combination of a several week long outburst (without evidence of repeated outbursts in the historical record), high absorption column (a large fraction of which is likely local to the system), and 11.82 s period does not fit neatly into existing X-ray binary categories.

Key words: accretion, accretion disks – binaries: close – stars: individual – X-rays: binaries

Online-only material: color figures

1. INTRODUCTION

One of the great contributions of the *INTEGRAL* satellite has been its scans of the Galactic plane and bulge, which have led to the discovery of a number of previously unknown transient X-ray binary sources (Bodaghee et al. 2007). Many of these sources have high columns of absorbing material along the line of sight, making the *INTEGRAL* hard X-ray response crucial for their discovery. In numerous cases a significant fraction of these columns are *intrinsic* to the systems in question. In fact, *INTEGRAL* has suggested possible interesting relationships between absorption and binary properties: a neutral column/orbital period anti-correlation (not unexpected as short periods increases the likelihood that an X-ray source is more deeply embedded within the wind/outflow from the secondary), and a neutral column/X-ray pulsar spin period correlation (which, if real, lacks an explanation; Bodaghee et al. 2007).

X-ray binaries themselves represent a wide variety of types of systems: high-mass X-ray binaries (HMXBs), which may be either wind fed or Roche lobe overflow fed, Be/X-ray binaries, and accreting millisecond X-ray pulsars (e.g., Paizis et al. 2005), among other types of systems. Outbursts can be very rapid, lasting only a few days in the case of the so-called supergiant fast X-ray transients (SFXTs; Negueruela et al. 2006; Sidoli 2011 and references therein), or last several weeks in the cases of Be/X-ray binaries and accreting millisecond X-ray pulsar systems. *INTEGRAL*, in combination with observations at other wavelengths, has been crucial in identifying the natures of these sources.

Since 2005 we have had a *Chandra*-followup program to observe previously unknown X-ray sources discovered by *INTEGRAL*, in order to aid in localizing and identifying these sources for multi-wavelength follow-up observations. On 2012 February 29 (MJD 55986) *INTEGRAL* discovered a new hard X-ray transient IGR J18179−1621 (Tuerler et al. 2012). The best source position was determined with the two JEM–X instruments with an associated uncertainty of $1\overset{'}{.}5$. The combined JEM–X and IBIS/ISGRI spectrum ($F_{3-50\,\rm keV} = 1.0 \times 10^{-9}$ erg cm^{-2} s^{-1}) could be described by a cutoff power law ($\Gamma = -0.5 \pm 0.5$, $E_{\rm cutoff} = 4.9^{+1.5}_{-0.9}$ keV, where photon flux per unit energy is $\propto E^{-\Gamma} \exp(-E/E_{\rm cutoff})$) plus a broad Gaussian absorption line ($E_{\rm c} = 20.8^{+1.4}_{-1.8}$ keV). According to the authors, if this line is interpreted as a cyclotron resonant scattering feature, IGR J18179−1621 could be an HMXB pulsar with a magnetic field of about 1.7×10^{12} G. The pulsating nature was confirmed by *Swift* and *Fermi*/GBM detections of a strong signal at $P = 11.82 \pm 0.01$ s (Halpern 2012; Li et al. 2012a; Finger & Wilson-Hodge 2012). The *Swift* observations performed on

February 29 confirmed the hard spectrum of IGR J18179−1621 ($\Gamma = 0.4 \pm 0.4$) as well as a high absorbing column density, $N_{\rm H} = (11.0 \pm 2.0) \times 10^{22}$ cm^{-2} (Li et al. 2012a).

A refined position with respect to the *INTEGRAL* discovery (1.′5 uncertainty) was reported by Li et al. (2012a) using *Swift* data. That position (2.″2 uncertainty) was consistent with the position measured by *INTEGRAL* and was compatible with an infrared candidate counterpart, 2MASS J18175218−1621316. However, this was not confirmed by Halpern (2012) who reported a *Swift*-based source position 4.″4 away (no error given), hence the proposed association with the Two Micron All Sky Survey (2MASS) source needed confirmation.

The day after the discovery of IGR J18179−1621, we triggered our approved *Chandra* target of opportunity program. The observation was originally set to occur on 2012 March 11, but due to a strong solar flare it was postponed until 2012 March 17. Thanks to the excellent *Chandra* imaging and astrometry, an X-ray position with a 0.″6 (90% confidence level) uncertainty was reported (Paizis et al. 2012). This new *Chandra*-based position was 0.″37 away from that obtained by Li et al. (2012a) and 0.″09 from the 2MASS J18175218−1621316 source ($K_s = 13.14$ mag). The preliminary *Chandra* position confirmed this latter source as the best candidate counterpart to IGR J18179−1621.

2. OBSERVATIONS AND DATA ANALYSIS

Since its discovery, IGR J18179−1621 has been observed by several X-ray observatories, i.e., *INTEGRAL*, *Swift*, and *Chandra*. In this paper we focus on our *Chandra* observations, but we include the recent *INTEGRAL* long-term light curve in order to place the *Chandra* observations within the overall context of the source outburst. Additionally, we consider quasi-simultaneous (within a few hours) *Swift* spectra. We refer to Bozzo et al. (2012) and Li et al. (2012b) for studies of the overall *Swift* and *INTEGRAL* data of IGR J18179−1621. We also report on our near-infrared (NIR) observations of the source field.

2.1. Chandra Data

We observed IGR J18179−1621 for 20 ks with *Chandra* from 2012 March 17, 23:09 UT to 2012 March 18, 05:17 UT (MJD 56003–56004, Observation ID 13684) with the High Energy Transmission Grating Spectrometer (HETGS; Canizares et al. 2000). The HETGS creates an undispersed, CCD-spectral resolution image (the 0th order), and creates high spectral resolution, dispersed spectra in the 0.8–10 keV band with the High Energy Grating (HEG) and in the 0.4–8 keV band with the Medium Energy Grating (MEG). The HEG and MEG contain multiple spectral orders, dispersed in opposite directions (positive and negative orders) along the *Chandra* CCD detectors. Throughout this work we shall consider data from the 0th order and the ±1st orders. Higher spectral orders have very low count rates, and thus shall be ignored.

Additionally, we consider a 16 ks archival *Chandra* observation, taken on 2007 February 11 (MJD 54142, Observation ID 6689), utilizing only the Advanced CCD Imaging Spectrometer-Imaging and -Spectroscopy arrays (ACIS-I and -S; i.e., the gratings were not utilized) that contained the position of IGR J18179−1621 within the ACIS-I field of view. We use these data to establish an upper limit to the X-ray flux of IGR J18179−1621 during an epoch prior to the outburst discussed in this work. (There are limited archival X-ray observations of IGR J18179−1621; see Bozzo et al. 2012 and Li et al. 2012b for further discussion of *Swift* and *INTEGRAL* observations.)

Both *Chandra* data sets were analyzed in a standard manner (with pixel randomization of the event positions turned off, and corrections for Charge Transfer Inefficiency in the CCD detectors applied) using the CIAO version 4.4 software package and *Chandra* CALDB version 4.4.8. The resulting spectra, which had integration times of 19.6 ks for the HETGS observation and 15.8 ks for the ACIS-I observation, were analyzed with the `ISIS` analysis system, version 1.6.1 (Houck 2002). Timing analysis of the data has been performed using the `S-lang/ISIS` Timing Analysis Routines[9] (`SITAR`) package.

2.2. INTEGRAL Data

Starting from its discovery, IGR J18179−1621 has been in the *INTEGRAL*/IBIS (Ubertini et al. 2003) field of view during the *inner Galactic disk*, *Galactic center* and *Scutum*/*Sagittarius arms* observations. A complete study of these *INTEGRAL* data is beyond the scope of this paper; however, in order to gauge the broadband long-term behavior of this source we have analyzed the IBIS/ISGRI (Lebrun et al. 2003) and JEM-X (Lund et al. 2003) data,[10] starting from revolution 1145 (2012 February 29, 02:20 UT, MJD 55986.1) to revolution 1153 (2012 March 25, 21:14 UT, MJD 56011.9). A standard analysis using version 9.0 of the Off-line Scientific Analysis (`OSA`) software was performed for the pointings where the source was in the JEM-X field of view and within 12° of the center of the IBIS/ISGRI field of view.

2.3. Swift Data

We analyzed two *Swift* observations performed on 2012 March 17, 15:02 UT, and 2012 March 18, 07:11 UT (ObsID 00032293013 and 00032293014). The *Swift*/XRT data were reduced with the `HEASOFT` suite v6.11 and the most recent calibration files available (XRT CALDB files released on 2012 March 21). Level 2 cleaned event files were produced from the raw data with `xrtpipeline` with standard parameters. The XRT was operated in photon counting mode and the observations amount to 1301 s and 1120 s of good time, respectively. XRT source spectra were then extracted from a 20 pixel radius circular region centered on the best source position obtained with *Chandra* (see Section 3.1.1). Background spectra were obtained from a source-free 40 pixel radius circular region. Ancillary response files were generated for both spectra with `xrtmkarf`, taking into account the exposure map at the source position. As no significant spectral variation was seen between the two observations, the spectra were co-added and fitted as a single spectrum together with the quasi-simultaneous *Chandra* spectra.

2.4. Near-infrared Data

Near-infrared K_s, H_n, and J_n observations were performed at the Universitätssternwarte Bochum near Cerro Armazones in the Chilean Atacama desert. We used the 80 cm IRIS telescope equipped with a 1024 × 1024 pixels HAWAII-1 detector array (Hodapp et al. 2010). The observational sequence consisted of eight exposures in each filter on two dates: H_n and K_s on 2012 March 13, 08:09–08:30 UT (MJD 55999.3) and K_s, H_n, and J_n on March 26 07:23–08:05 UT (56012.3), each comprising conventional dithering and chopping patterns to allow subtraction

[9] http://space.mit.edu/CXC/analysis/SITAR/

[10] We have analyzed available JEM-X1 and JEM-X2 data, but as they are consistent, we show only JEM-X1 results for clarity.

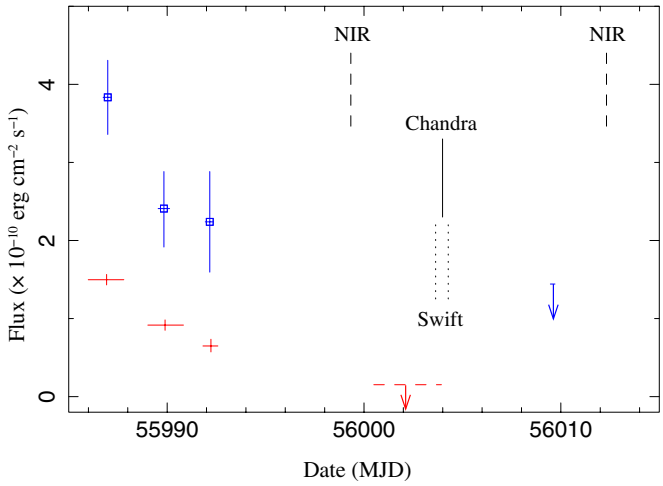

Figure 1. X-ray light curves of IGR J18179−1621 as seen by *INTEGRAL* from its discovery (red crosses for IBIS/ISGRI, 18–40 keV, and blue squares for JEM-X1, 3–10 keV). Upper limits in the last observations are shown (1.5×10^{-11} erg cm^{-2} s^{-1} $\approx$ 1.6 mCrab, for IBIS/ISGRI, and 1.5×10^{-10} erg cm^{-2} s^{-1} $\approx$ 9 mCrab, for JEM-X1). The vertical lines show the times of the *Chandra* observation (solid line), the two quasi-simultaneous *Swift* observations (dotted lines), and the NIR observations (dashed lines) studied in this paper.

(A color version of this figure is available in the online journal.)

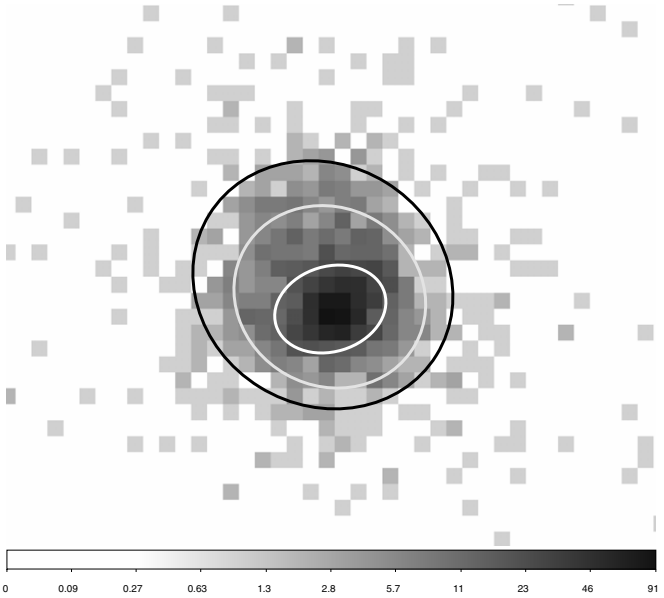

Figure 2. *Chandra* 0th order image for IGR J18179−1621, using ≈1/8″ pixels. The image has been rotated so that the spacecraft +*Z* coordinate points upward, and the expected *Chandra* PSF anomaly should lie in the upper left of this image. The white (inner) and black (outer) lines are the 2σ contours of the double 2D Gaussian fit to this image, while the gray (middle) line is the 2σ contour for the best-fit single 2D Gaussian.

of the bright NIR sky. The total on-source integration time was 400 s in each filter. Data reduction involved standard IRAF procedures; astrometric and photometric calibration were achieved via nearly 2400 and 700 sources, respectively, from the 2MASS archive.

We also have obtained archival data from the United Kingdom Infrared Telescope (UKIRT) Infrared Deep Sky Survey (UKIDSS; see Lawrence et al. 2007, and Casali et al. 2007; Hewett et al. 2006; Hodgkin et al. 2009; Hambly et al. 2008 for a description of the instruments, calibration, and pipeline). The source is detected during three epochs: Epoch 2006 05 01, with $H = 16.45 \pm 0.03$ mag; Epoch 2006 07 07, with $H = 16.70 \pm 0.03$ mag and $K = 13.007 \pm 0.003$ mag; and Epoch 2007 08 22, with $K = 13.043 \pm 0.004$ mag. There are no J-band detections of this source in the UKIDSS database. Below, we compare these results to our recent NIR measurements.

3. RESULTS

The X-ray (3–10 keV and 18–40 keV) light curves of the 2012 outburst of IGR J18179−1621 as seen by *INTEGRAL*/JEM-X1 and *INTEGRAL*/IBIS, respectively, are presented in Figure 1. The first three data points are the average fluxes in *INTEGRAL* revolutions 1145, 1146, and 1147, shown as red crosses for IBIS/ISGRI and blue squares for JEM-X1.[11] Upper limits in the last observations are shown: IBIS/ISGRI upper limit (1.5×10^{-11} erg cm^{-2} s^{-1} $\approx$ 1.6 mCrab at 5σ, ∼300 ks) in revolutions 1150–1153 and the JEM-X1 upper limit (1.5×10^{-10} erg cm^{-2} s^{-1} $\approx$ 9 mCrab at 3σ, ∼22 ks) in revolution 1153. In all cases, the shorter exposure times of JEM-X with respect to IBIS/ISGRI are due to the smaller field of view. We refer to Bozzo et al. (2012) for a soft X-ray (0.3–10 keV) *Swift* light curve of the source outburst and for a combined *INTEGRAL–Swift* spectral study of *INTEGRAL* revolutions 1145, 1146, and 1147. In Figure 1, the solid line shows the time of our 20 ks *Chandra* observation while the two dashed lines refer to the times of the two quasi-simultaneous *Swift* observations analyzed in this paper.

3.1. Chandra

3.1.1. Chandra position

We determine the X-ray position of IGR J18179−1621 using the *Chandra* 0th order image, finding $\alpha_{J2000} = 18^h17^m52\overset{s}{.}18$, $\delta_{J2000} = -16°21'31\overset{''}{.}68$. This position is 0$\overset{''}{.}$143 from the one we reported in Paizis et al. (2012), which was obtained from the `tgdetect` tool which fits a single, two-dimensional (2D) Gaussian to the 0th order image. This shift with respect to the position reported in Paizis et al. (2012) is due to the fact that in this work we have more accurately taken into account a known artifact[12] in the *Chandra* point-spread function (PSF) by fitting the 0th order image with two asymmetric 2D Gaussian functions. The broader Gaussian function is sensitive to the expected PSF anomaly, while the narrower Gaussian function is fit to the core of the PSF. The asymmetry of the broad component of the PSF is seen in Figure 2. This PSF anomaly is very rarely noticeable, as it can be unveiled only when the source is bright enough to map it, but not so bright as to distort the resulting PSF shape due to the effects of pileup. The centroid of the narrow Gaussian function is taken as the position of IGR J18179−1621. Since the statistical errors for the parameters of this narrow Gaussian are smaller than the absolute pointing accuracy of *Chandra*, 0$\overset{''}{.}$6 at 90% uncertainty,[13] and since there are no other point sources within this *Chandra* observation's field of view to refine further the astrometry, we attribute a 90% confidence level uncertainty of 0$\overset{''}{.}$6 to the above reported position.

[11] Revolution 1148 included *inner Galactic disk* observations that could not be used due to an intense solar flare that caused a very high radiation environment around *INTEGRAL* and forced the JEM-X and IBIS/ISGRI instruments into safe modes.

[12] http://cxc.harvard.edu/ciao4.4/caveats/psf_artifact.html

[13] http://cxc.harvard.edu/cal/ASPECT/celmon/

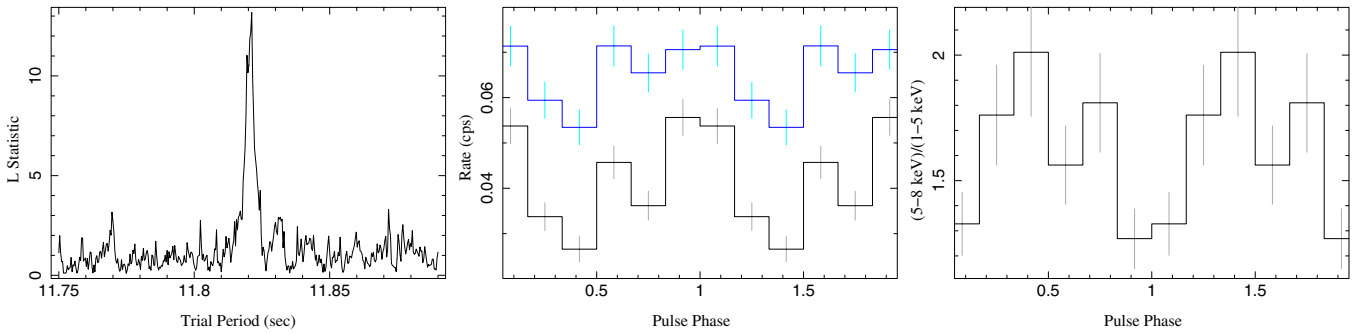

Figure 3. Left: epoch fold (Davies 1990) significance statistic (using six phase bins) of the *Chandra* 0th order, barycenter-corrected light curve of IGR J18179−1621. The peak period is 11.821 s. Middle: the 0th order rate, as a function of pulse phase, in the 1–5 keV band (bottom curve) and the 5–8 keV band (top curve). Right: the ratio of the 5–8 keV to 1–5 keV rates as a function of pulse phase.

(A color version of this figure is available in the online journal.)

3.1.2. Chandra Variability: the Pulsation of IGR J18179−1621

Periodic variability of the IGR J18179−1621 X-ray light curve was first reported by Halpern (2012) who used *Swift* observations to detect an 11.82 ± 0.01 s period and a pulsed fraction of 27% in the 2–10 keV band. Such a periodicity is within the realm of detectability with our *Chandra* observations, which had a nominal frame time of 1.84104 s: a 1.8 s exposure, followed by a 41.04 ms CCD readout. Actually, due to (expected and corrected on the ground) clock drifts, the mean frame time for our observation was 1.84121 s. To search for the reported periodicity in IGR J18179−1621, we barycentered the light curve and then performed an epoch fold (Davies 1990) of this light curve using six phase bins for the trial periods. We chose six phase bins since, with the reported period; this gave folded light-curve bin durations comparable to the frame time. When folding the light curve, an X-ray event is placed wholly into a single phase bin if its barycentered time (which corresponds to the middle of the *Chandra* integration frame time) falls anywhere within that phase bin. That is, we do not add any randomization within a frame time to an event (which would tend to smear out a signal), and we do not assign fractional events across phase bins (which would introduce artificial correlations among bins). Although we are working near the *Chandra* temporal resolution, the fact that we sample nearly 1700 pulse periods suggests that we should be able to determine the pulse period to an accuracy of the order of 0.01 s.

In Figure 3 (left panel), we show the results of an epoch fold of the 0th order 1–8 keV light curve, extracted from a 4 pixel radius around the point source, where we have searched 400 equally spaced trial periods between 11.75 and 11.89 s. We see that there is a strongly detected signal at 11.82 s, in agreement with the results of Halpern (2012). The significance of this period (ignoring the number of trials) is nominally $p = 6 \times 10^{-6}$, compared to the significances for the bulk of the trial values which are $p \gtrsim 0.1$. Folding the light curve on the most significant period (Figure 3, middle panel), we see that the 1–5 keV X-rays show greater modulation than the 5–8 keV light curve. The standard deviation is 27% of the mean for the former, and 11% of the mean for the latter. Looking at the colors of the folded light curve, we see that the light curve softens at the peak of the pulse (Figure 3, right panel). (With a mean count rate of 0.24 counts/integration frame, the 0th order light curve is slightly affected by photon pileup, which will tend to harden the pulse peak, not soften it. Additionally, pileup will tend to slightly decrease the fractional amplitude of the pulse modulation.)

3.1.3. Quasi Simultaneous Swift–Chandra Spectra

Although the folded X-ray light curves show evidence for a mild spectral softening during the pulse peak, we lack the statistics to describe this variation with spectral fits. We therefore only present fits to the mean spectrum. We choose to fit the near contemporaneous *Swift* spectra simultaneously with the *Chandra* spectra, and in fact we do not even require a cross-normalization constant between these two sets of spectra. All spectra discussed below have been binned to a signal-to-noise ratio of 4.5 and noticed only in the 2–8 keV band.

We find that a simple model fits the spectra well: an absorbed power law. We describe the absorption using the model, `TBnew`, and abundances derived from Wilms et al. (2000). This model results in higher column densities with respect to, e.g., the `wabs` model using the cross-sections and abundances of Morrison & McCammon (1983). Indeed, in earlier interstellar medium (ISM) absorption models the assumed ISM abundances were solar, while measurements outside the solar system showed that the total gas plus dust ISM abundances are actually lower than solar abundances. Hence, with this correction, a higher column density is needed for a given spectrum (Wilms et al. 2000 and references therein).

We further apply a pileup model (Davis 2001) to the 0th order data, although the pileup parameter, α, which determines the probability of a piled event being detected as a "good event" is completely undetermined within its allowed range of 0–1. This is not unexpected as a power-law spectrum when piled appears as a slightly harder power law. The uncertainty in the α parameter merely serves to widen the error bars on the fitted spectral slope, Γ.

The fitted neutral column is large, $N_{\rm H} = (2.2 \pm 0.3) \times 10^{23}$ cm^{-2} (90% confidence level). The fitted photon index is extremely hard: $\Gamma = 0.4 \pm 0.1$ (90% confidence level). The fitted absorbed 2–8 keV flux is $(1.41 \pm 0.07) \times 10^{-11}$ erg cm^{-2} s^{-1} (90% confidence level), i.e., $L^{\rm abs}_{2-8\,{\rm keV}} \approx 10^{35}$ erg s^{-1} if the source is at 8 kpc and isotropically emitting. The χ^2 of the fit is 137.7 for 143 degrees of freedom. We present these fits in Figure 4. There is no strong evidence for any spectral complexity beyond an absorbed power law. One can add a narrow Fe Kα line to the spectra and find a 30 eV equivalent width (EW), but the 90% confidence level error bars of this line encompass 0 eV EW and are limited to $\leqslant$71 eV EW.

The *Swift* spectra agree reasonably well with the *Chandra* spectra, within their limited statistics. If fit on their own, the *Swift* spectra prefer a softer power law ($\Gamma = 1.2^{+1.7}_{-1.2}$, $\chi^2 = 8.8$ for 7 degrees of freedom); however, all spectral

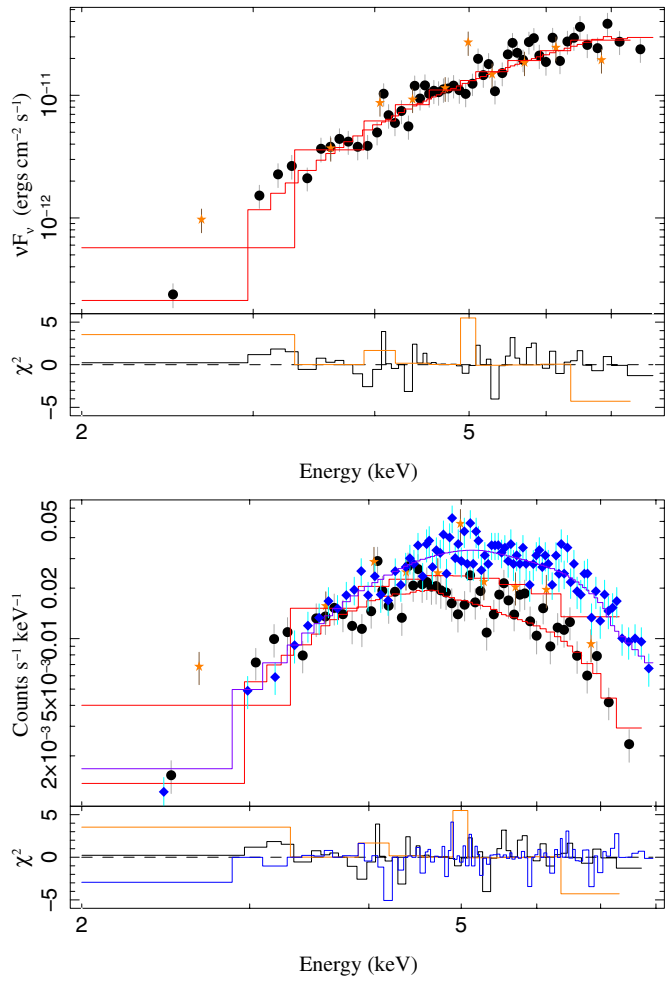

Figure 4. Top: flux-corrected spectra for the combined ±1st order HETG (black circles) and *Swift* (orange stars) spectra of IGR J18179−1621, fit with an absorbed power law. Bottom: detector space spectra of IGR J18179−1621 for the combined ±1st order HETG, *Swift*, and 0th order (blue diamonds), fit with an absorbed power law. (Additionally, a pileup model has been applied to the 0th order spectra.)

(A color version of this figure is available in the online journal.)

parameters from the *Swift*-only fits have 90% confidence level error bars that overlap the best-fit parameters of the joint fit. Specifically, $N_{\rm H} = (2.3^{+1.9}_{-1.1}) \times 10^{23}\,{\rm cm}^{-2}$, absorbed 2–8 keV flux $= (1.29 \pm 0.20) \times 10^{-11}\,{\rm erg\,cm}^{-2}\,{\rm s}^{-1}$.

The above results are to be compared to the flux limits obtained from the archival *Chandra*/ACIS-I observation of 2007 February 11. We extract events in a 25″ radius region (chosen this large to encompass the off-axis *Chandra* point spread function) centered on the position of IGR J18179−1621, and background events from a nearby 115″ radius, apparently source-free region. In the 2–9 keV band there are 38 detected events, compared to an expected 31 events from the measured background (i.e., there is a 1σ excess of events). Using the same best-fit model for the *Chandra*/*Swift* data, but leaving the model normalization free, the 90% confidence level upper limit to the 2–8 keV source flux during this observation is $1.6 \times 10^{-13}\,{\rm erg\,cm}^{-2}\,{\rm s}^{-1}$. Thus, we see that quiescent X-ray flux levels of IGR J18179−1621 can be at least 87 times fainter than the flux level found with the recent *Chandra*-HETGS and *Swift* observations.

Searching 2.4 Ms of IBIS/ISGRI observations and 410 ks of JEM-X observations of this field of view performed between 2003 February 28 and 2010 March 1, Bozzo et al. (2012) did not detect IGR J18179−1621. The 5σ upper limits for the mean source flux over these observations were 0.5 mCrab ($\approx 5 \times 10^{-12}\,{\rm erg\,cm}^{-2}\,{\rm s}^{-1}$) in the IBIS/ISGRI band and 1.7 mCrab ($\approx 2.7 \times 10^{-11}\,{\rm erg\,cm}^{-2}\,{\rm s}^{-1}$) in the JEM-X band. The latter, covering the 3–10 keV band, is actually slightly higher than our *Chandra*-HETGS detection and significantly higher than the 90% confidence level upper limits provided by the ACIS-I observation. Still, these limits show that flux levels comparable to the beginning of the outburst seen in Figure 1 have not been typical in *INTEGRAL* observations of IGR J18179−1621.

3.2. Near-infrared

The final averaged K_s, H_n, and J_n images of the field of view around IGR J18179−1621, taken on 2012 March 13, are shown in Figure 5 and display sources down to magnitudes $K_s \sim 16$ mag, $H_n \sim 17$ mag, and $J_n \sim 18$ mag.

At the *Chandra* position of the source (0.″09 away), there is the previously discussed 2MASS J18175218−1621316 (inner most red circle in Figure 5) with an observed brightness on 2012 March 13 of $K_s = 13.14 \pm 0.04$ mag, $H_n = 16 \pm 0.1$ mag, and no counterpart in the J_n band, with $J_n > 18$ mag. The source shows no evidence of NIR variability between 2012 March 13 and 26.

The above observations are to be compared to the results from UKIDSS. Although the UKIDSS database shows a 0.25 mag variation in H, the IR source is quite faint and is likely contaminated by a close by, brighter source (see Figure 5, middle panel). There is little variation among the K-band detections of UKIDSS (K =13.007–13.043 mag), 2MASS (K_s =13.14 mag), and IRIS (K_s =13.14 mag). The epochs of the UKIDSS K-band measurements bracket the *Chandra*/ACIS-I quiescent observation, while our IRIS observation was taken during the outburst of IGR J18179−1621, yet these NIR observations are all consistent with one another. Also consistent with our recent observations, UKIDSS did not detect IGR J18179−1621 in the J band.

4. DISCUSSION

4.1. IGR J18179−1621: X-Ray/NIR

2MASS J18175218−1621316 (inner red circle in Figure 5) is the only source from the 2MASS All-Sky Point Source Catalog that is within 1″ of the *Chandra*-determined position of IGR J18179−1621, and the 2MASS point-source density within 60″ of this position is 0.01 arcsec^{-2}. Given that the *Chandra* error circle for IGR J18179−1621 is $\approx$1 arcsec^2, the simplest hypothesis is that this 2MASS source (with a $\sim$0.1″ error radius) is the actual NIR counterpart to the X-ray source. There still remains, however, an $\gtrsim$1% probability that the 2MASS source is a chance coincidence. As we discuss in Section 4.2, if IGR J18179−1621 lies between 1 and 10 kpc distant, a wide range of companion types plausibly would have NIR flux levels and colors of this 2MASS source, even in the presence of large extinction. In what follows, we therefore adopt the hypothesis that 2MASS J18175218−1621316 is indeed the NIR counterpart to IGR J18179−1621.

The 2MASS catalog provides a source K magnitude of 13.14 ± 0.04 mag, to be compared to our constant NIR observed 13.14 ± 0.04 mag and the UKIDSS K magnitude of 13.007–13.043 mag. Hence, though the X-ray outburst decay inferred from *Swift* monitoring ($\sim$22 days, Bozzo et al. 2012; Li et al. 2012b) may resemble a low-mass X-ray binary outburst

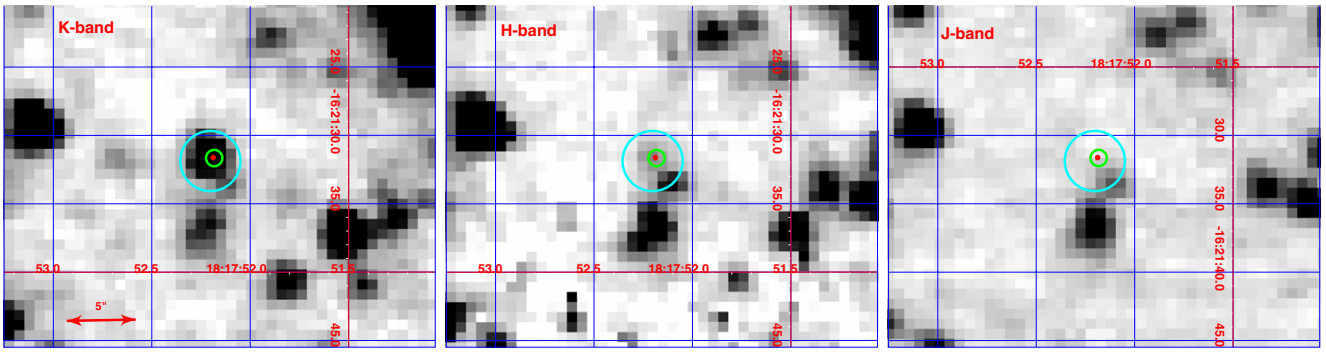

Figure 5. K_s (left), H_n (middle), and J_n (right) band images of the field of view of IGR J18179−1621 taken on 2012 March 13. In both images we over-plot the *Swift*/XRT 90% error circle, 2.″2 radius (cyan; Li et al. 2012a) and the *Chandra* 90% error circle, 0.″6 radius (green; this paper). The position of the 2MASS J18175218 − 1621316 candidate (in red, 1σ, 0.″11 radius) lies entirely within the *Chandra* error circle.

(A color version of this figure is available in the online journal.)

type of event (accretion disk instability), the essentially constant level of the NIR emission (in the 2MASS and UKIDSS catalogs and in our observations during the outburst) suggests that we are seeing the stable high-mass companion at $K_s \sim 13$ mag. The J-band upper limits from our observations and UKIDSS further indicate that this companion is highly obscured.

The heavily absorbed ($N_{\rm H} = (2.2 \pm 0.3) \times 10^{23}\,{\rm cm}^{-2}$) and hard spectrum ($\Gamma = 0.4 \pm 0.1$) obtained in the joint *Chandra–Swift* spectral fit (Section 3.1.3), together with the 11.82 s pulsation (Section 3.1.2) and the putative cyclotron line discussed by Bozzo et al. (2012) and Li et al. (2012b) point to an identification of IGR J18179−1621 as an HMXB hosting a neutron star (NS).

The expected neutral column along this line of sight is $\approx 10^{22}\,{\rm cm}^{-2}$ (Dickey & Lockman 1990; Kalberla et al. 2005), which is more than a factor of 10 smaller than the measured column. A substantial fraction of the measured neutral column is therefore likely local to the system and associated with an atmosphere/wind/accreting matter coming from the secondary. Associated with this local absorption we expect an Fe Kα emission line with EW $\approx 3.3\,(N_{\rm H}/10^{22}\,{\rm cm}^{-2})$ eV $\approx$ 73 eV, as has been found empirically in *Chandra* studies of HMXBs (Torrejón et al. 2010). Such a Fe line strength is also expected under the approximation that the obscuring material is spherically distributed about the X-ray source (Kallman et al. 2004). Monte Carlo simulations of a power-law source embedded within an absorbing cloud show the line equivalent width to be between 50 eV and 100 eV for material of solar and twice solar abundances (Eikmann 2012, private communication). For these reasonable assumptions, the lack of a detectable Fe Kα line is therefore consistent with the expectations and it can be assumed that the bulk of the observed neutral column is local to the system.

Figure 3 (middle and right panels) shows that the softer 1–5 keV folded light curve has greater modulation than the harder 5–8 keV light curve. That is, the light curve softens at the peak of the 11.82 s pulse. Such an energy dependent pulse profile is seen in many magnetized neutron stars, where the stronger variability at lower energies is typically attributed to absorption in the accretion column, while the (typically sinusoidal) emission pattern at harder energies is due to emission from the bottom of the accretion column (Caballero et al. 2011 and references therein).

4.2. The Nature of IGR J18179−1621: an HMXB?

HMXBs are known to be divided into different groups according to the nature of the companion, formation and

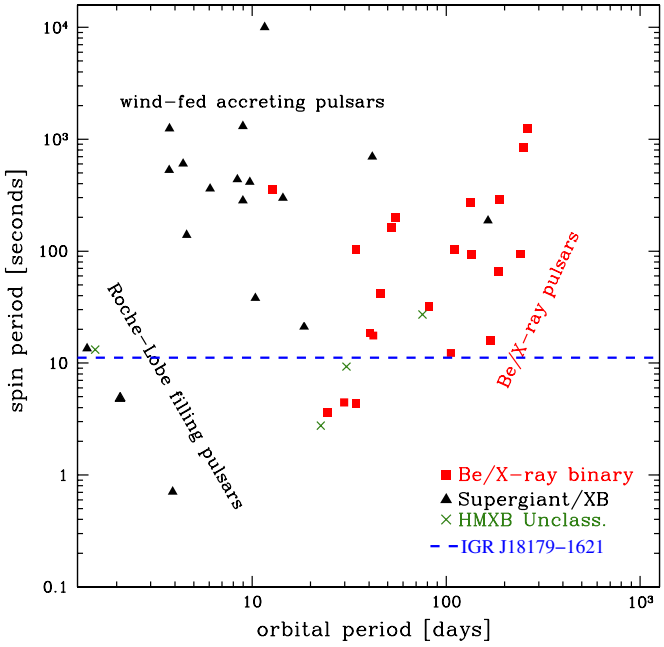

Figure 6. Corbet diagram (NS $P_{\rm spin}$ vs. system $P_{\rm orb}$; Corbet 1986) showing the three HMXB populations: BeHMXB, sgHMXB Roche lobe overflow, and sgHMXB-wind fed. See the text. IGR J18179−1621 ($P_{\rm orb}$ unknown) lies along the horizontal blue line at $P_{\rm spin} \sim 12$ s. Adapted from a figure by J. A. Zurita Heras, as originally presented by Chaty (2011).

(A color version of this figure is available in the online journal.)

geometry of the system (e.g., Chaty 2011 and references therein). They include BeHMXB X-ray transients, usually hosting an NS on a wide eccentric orbit around a B0–B2e spectral type donor star with a decretion disk; and supergiant HMXBs (sgHMXBs), hosting an NS on a circular orbit around a supergiant OB star. sgHMXBs can be either Roche lobe overflow sources (RLO; rare transient sources with outburst luminosities of $L_{\rm X} \sim 10^{38}\,{\rm erg\,s}^{-1}$), or wind-fed systems (e.g., the majority of sgHMXBs, with persistent luminosities of $L_{\rm X} \sim 10^{35-36}\,{\rm erg\,s}^{-1}$).

An efficient way to visualize all such sources is via the so-called Corbet diagram (Corbet 1986), where the NS spin period, $P_{\rm spin}$, is plotted versus the system orbital period, $P_{\rm orb}$ (Figure 6). In general, in such a diagram BeHMXBs populate the region with higher $P_{\rm orb}$ (roughly $P_{\rm orb} > 20$ days), while sgHMXBs populate the lower part ($P_{\rm orb} < 20$ days). $P_{\rm spin}$ ranges from about 1 s to 10^3 s for both classes of sources (Figure 6; see also

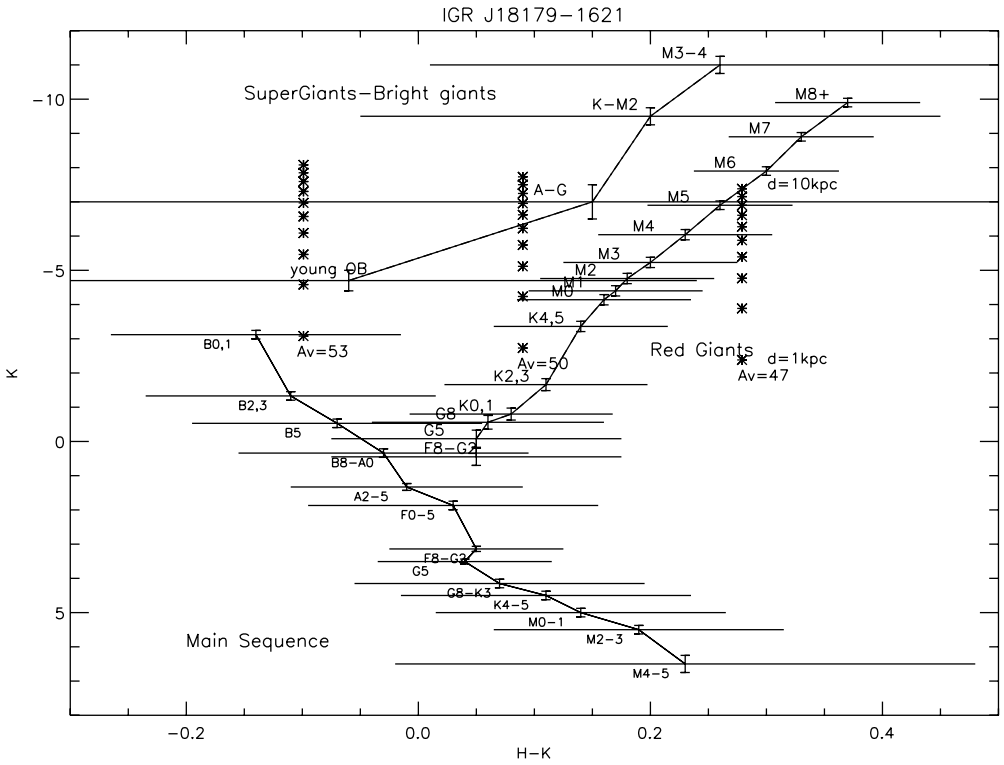

Figure 7. Plot of expected $H-K$ colors vs. absolute K magnitude for different stellar types. Superimposed on this are points (asterisks) for the NIR measurements of IGR J18179−1621, assuming three different visual extinctions (A_V =47, 50, and 53 mag) for assumed distances ranging from 1 to 10 kpc.

Chaty 2011; Sidoli 2011). The majority of transient sources with spin periods $\lesssim$20 s are in fact BeHMXBs.

In the last decade, two new classes of wind accreting pulsars in sgHMXBs have been discovered (Bodaghee et al. 2007): obscured, fairly persistent sources with a huge intrinsic local extinction, and sgHMXBs exhibiting fast and transient outbursts, known as SFXTs (see e.g., Sidoli 2011 for a recent review, especially Figure 2 therein). The neutral column of IGR J18179−1621 is typical of this latter category of sources, but its spin period—and prolonged outburst—is not.

Based on the above discussion, IGR J18179−1621 does not clearly fall into any of the above classes. Its transient nature seems to exclude the highly obscured and standard wind-fed systems that are fairly persistent. A few week-long transient outburst of IGR J18179−1621 could suggest that it is a BeHMXB, with its 11.82 s spin period placing it at the lower end of orbital periods in the Corbet diagram, i.e., several tens of days (20–80 days). Although many Be X-ray binaries show periodic outbursts, many other Be show long periods of quiescence. A good example is A0535+26, which has had only five major outburst phases since its 1975 discovery, which were separated by many years of quiescence (e.g., between 1994 February and 2005 May; see Caballero et al. 2007 and references therein).

On the other hand, despite its transient nature IGR J18179−1621 would be unusual for an SFXT, since these sources are known to have very fast outbursts, on the order of hours or a few days at most, as seen by *INTEGRAL*/IBIS. Figure 1 shows that IGR J18179−1621 is detected for at least three revolutions, i.e., about 12 days. An extremely nearby SFXT, however, may not be excluded.

RLO sources, i.e., transient sgHMXBs strictly filling their Roche lobe (pure accretion disk accretors) are rare, since the mass transfer is highly unstable and the accretion should only last for a few thousand years. Instead, there are HMXBs exhibiting beginning atmospheric Roche lobe overflow, where the massive star does not fill its Roche lobe, but the stellar wind follows the Lagrange equipotentials, and accumulates, forming an accretion disk (Bhattacharya & van den Heuvel 1991). This situation is more stable, but still rare due to the required configuration of stellar radius, orbital distance and mass ratio. We know only three such systems in total, hosting NSs: LMC X-4, Cen X-3, and SMC X-1. IGR J18179−1621 could be the fourth source belonging to this class.

Finally, we consider the possible stellar companions in IGR J18179−1621, based on the NIR measurements coupled with assumptions about possible distances and assumed extinctions. In Figure 7, we show absolute K-magnitude versus $H-K$ colors, for a series of stellar sequences. Overplotted on this are the absolute K-magnitude and $H-K$ colors for the counterpart of IGR J18179−1621 given our measurements, and assuming distances ranging from 1 to 10 kpc.

We estimate the extinction toward the source from the relationship of Predehl & Schmitt (1995), modified to account for the fact that absorption model of Wilms et al. (2000) fits neutral columns ≈30% larger than the model used by Predehl & Schmitt (1995). Specifically, we assume $A_V \sim N_H/2.7 \times 10^{21}\,\mathrm{cm}^{-2}$. The 21 cm column translates to an extinction of $A_V = 3.7$ mag, while the full-fitted neutral column yields $A_V \sim 82$ mag. Note, however, that the Predehl & Schmitt (1995) relationship is based on measurements of X-ray dust scattering halos. Source intrinsic absorption in the stellar wind would happen in a medium that does not contain dust and thus for such a case the Predehl & Schmitt (1995) relationship overestimates the A_V.

Figure 7 shows that the range of extinctions from A_V = 47–52 mag is the only range where our NIR measurements

intersect standard stellar sequences. While IGR J18179−1621 could be consistent with a low-mass X-ray binary (LMXB), with a red giant companion ranging from K-type ($A_V \sim 49$, at 1 kpc) to M-type ($A_V \sim 47$, at 10 kpc), an LMXB nature seems unlikely, given the 11.82 s pulsation and very hard X-ray spectrum of IGR J18179−1621. More realistic models for IGR J18179−1621 are that it is an HMXB. Supergiant companions can range from a close by OB-type ($A_V \sim 52$, at 2 kpc) to a further away A-type ($A_V \sim 49$, at 7 kpc). Even a nearby B-type main-sequence star is allowed ($A_V \sim 52$), at 1 kpc.

In all these cases, A_V is ∼50% of what is obtained by calculating A_V from the X-ray N_H. This result argues that about half of the observed column is caused by the neutron star being embedded in the stellar wind of an early-type donor, while the other half of the column would be in the (dusty) ISM close to the binary. The deduced column for the wind absorption, $N_{H,wind} \sim 10^{23}$ cm^{-2}, is consistent with that seen in a number of HMXBs. For example, the XRB GX 301−2, which orbits a B1 Ia hypergiant in a 41.5 d elliptical orbit, has an N_H that is strongly variable, with $N_H \sim 10^{24}$ cm^{-2} during the pre-periastron flare (Fürst et al. 2011) and $N_H \sim 10^{23}$ cm^{-2} and lower after the periastron passage (Suchy et al. 2012). Unfortunately, we lack detailed observations over the course of the outburst that might have revealed variations of the neutral column. The nature of IGR J18179−1621 at this time still remains ambiguous.

We thank the *Chandra* team for its rapid response in scheduling and delivering the observation, as well as the *INTEGRAL* Science Data Center for its quick and efficient sharing of *INTEGRAL* results. A.P. thanks Enrico Bozzo for useful discussion and for the support in the early phases of the source outburst that led to the *Chandra* trigger. We thank the referee for comments that improved this manuscript. M.A.N. acknowledges the support of NASA grants GO2-13035X and SV3-73016. M.D.S. acknowledges financial contribution from the agreement ASI-INAF I/009/10/0 and from PRIN-INAF 2009 (PI: L. Sidoli). V.G. and J.W. acknowledge support by the Bundesministerium für Wirtschaft und Technologie under Deutsches Zentrum für Luft- und Raumfahrt grant 50 OR 1113. This paper is partly based on observations with *INTEGRAL*, an ESA project with instruments and science data center funded by ESA member states, Czech Republic and Poland, and with the participation of Russia and the USA. This research has made use of the *INTEGRAL* sources page http://irfu.cea.fr/Sap/IGR-Sources/ and the *INTEGRAL* Spiral Arm pages http://sprg.ssl.berkeley.edu/∼bodaghee/isa/. This publication makes use of data products from the Two Micron All Sky Survey, which is a joint project of the University of Massachusetts and the Infrared Processing and Analysis Center/California Institute of Technology, funded by the National Aeronautics and Space Administration and the National Science Foundation. A.P. and P.U. acknowledge financial contribution from the ASI-INAF agreement I/033/10/0.

REFERENCES

Bhattacharya, D., & van den Heuvel, E. P. J. 1991, Phys. Rep., 203, 1
Bodaghee, A., Courvoisier, T. J.-L., Rodriguez, J., et al. 2007, A&A, 467, 585
Bozzo, E., Ferrigno, C., Türler, M., Manousakis, A., & Falanga, M. 2012, A&A, in press
Caballero, I., Kraus, U., Santangelo, A., Sasaki, M., & Kretschmar, P. 2011, A&A, 526, A131
Caballero, I., Kretschmar, P., Santangelo, A., et al. 2007, A&A, 465, L21
Canizares, C. R., Huenemoerder, D. P., Davis, D. S., et al. 2000, ApJ, 539, L41
Casali, M., Adamson, A., Alves de Oliveira, C., et al. 2007, A&A, 467, 777
Chaty, S. 2011, in ASP Conf. Ser. 447, Evolution of Compact Binaries, ed. L. Schmidtobreick, M. R. Schreiber, & C. Tappert (San Francisco, CA: ASP), 29
Corbet, R. H. D. 1986, MNRAS, 220, 1047
Davies, S. R. 1990, MNRAS, 244, 93
Davis, J. E. 2001, ApJ, 562, 575
Dickey, J. M., & Lockman, F. J. 1990, ARA&A, 28, 215
Finger, M. H., & Wilson-Hodge, C. A. 2012, ATel, 3961
Fürst, F., Suchy, S., Kreykenbohm, I., et al. 2011, A&A, 535, A9
Halpern, J. P. 2012, ATel, 3949
Hambly, N. C., Collins, R. S., Cross, N. J. G., et al. 2008, MNRAS, 384, 637
Hewett, P. C., Warren, S. J., Leggett, S. K., & Hodgkin, S. T. 2006, MNRAS, 367, 454
Hodapp, K. W., Chini, R., Reipurth, B., et al. 2010, Proc. SPIE, 7735, 77351A
Hodgkin, S. T., Irwin, M. J., Hewett, P. C., & Warren, S. J. 2009, MNRAS, 394, 675
Houck, J. C. 2002, in Proc. of High Resolution X-Ray Spectroscopy with XMM-Newton and Chandra, ed. G. Branduardi-Raymont, 17
Kalberla, P. M. W., Burton, W. B., Hartmann, D., et al. 2005, A&A, 440, 775
Kallman, T. R., Palmeri, P., Bautista, M. A., Mendoza, C., & Krolik, J. H. 2004, ApJ, 155, 675
Lawrence, A., Warren, S. J., Almaini, O., et al. 2007, MNRAS, 379, 1599
Lebrun, F., Leray, J. P., Lavocat, P., et al. 2003, A&A, 411, L141
Li, J., Zhang, S., Chen, Y. P., et al. 2012a, ATel, 3950
Li, J., Zhang, S., Torres, D., et al. 2012b, MNRAS, 1313
Lund, N., Budtz-Jørgensen, C., Westergaard, N. J., et al. 2003, A&A, 411, L231
Morrison, R., & McCammon, D. 1983, ApJ, 270, 119
Negueruela, I., Smith, D. M., Reig, P., Chaty, S., & Torrejón, J. M. 2006, in The X-Ray Universe 2005, ed. A. Wilson (ESA Special Publication, Vol. 604; Noordwijk: ESA), 165
Paizis, A., Nowak, M., Rodriguez, J., et al. 2012, ATel, 3988
Paizis, A., Nowak, M. A., Wilms, J., et al. 2005, A&A, 444, 357
Predehl, P., & Schmitt, J. H. M. M. 1995, A&A, 293, 889
Sidoli, L. 2011, in Proceedings of "The Extreme and Variable High Energy Sky," Vol. PoS(extremesky 2011)010, Proceedings of Science (PoS), http://pos.sissa.it/cgi-bin/reader/conf.cgi?confid=147
Suchy, S., Fürst, F., Pottschmidt, K., et al. 2012, ApJ, 745, 124
Torrejón, J. M., Schulz, N. S., Nowak, M. A., & Kallman, T. R. 2010, ApJ, 715, 947
Tuerler, M., Chenevez, J., Bozzo, E., et al. 2012, ATel, 3947
Ubertini, P., Lebrun, F., Di Cocco, G., et al. 2003, A&A, 411, L131
Wilms, J., Allen, A., & McCray, R. 2000, ApJ, 542, 914